Thickness-dependent valence-band photoemission from thin InAs and GaAs films

H. Åsklund, L. Ilver, J. Kanski, and S. Mankefors

Department of Experimental Physics, Chalmers University of Technology and Göteborg University, SE-412 96 Göteborg, Sweden

U. Södervall

*Department of Microelectronics and Nanoscience, Chalmers University of Technology and Göteborg University,
SE-412 96 Göteborg, Sweden*

J. Sadowski

*MAX-lab, Lund University, SE-221 00 Lund, Sweden
and Institute of Physics, Polish Academy of Sciences, 02-668 Warsaw, Poland*

With the aim to follow the development of the electronic properties in thin films, angle-resolved photoelectron spectroscopy has been used to investigate molecular beam epitaxy grown InAs layers on GaAs(111)*A* and GaAs layers on AlAs(100), lattice mismatch 7.2% and 0.1%, respectively. The results show that the bulk electronic structure in the overlayer material is established only in films thicker than 3–4 nm and that the interface region in effect displays alloylike electronic properties even though the interface is geometrically abrupt. Comparing computations of strain effects on the electronic structure in bulk InAs with the experimental data on the InAs cap layers, it was possible to separate the contributions of geometrical strain effects, extending 5–6 nm into the overlayer, and the electronic interface effects, extending 3–4 nm.

I. INTRODUCTION

A general feature in current multilayer-based semiconductor device fabrication is progressive miniaturization. Detailed knowledge about the interface regions thus becomes of vital importance. Since the electronic properties are determined by the atomic arrangement, much work has been devoted to studies of the interface structure and chemistry. As to the electron structure itself, there are numerous investigations focused on band offsets or electronic coupling in quantum well (QW) structures,[1,2] but relatively little attention has been given to further characterization of the electron states in the interface region. The relevance of a more extensive characterization of the heterointerfacial electronic properties is stressed, for example, by the results of a detailed scanning tunneling spectroscopy (STS) study of GaAs/Al_xGa_{1-x}As(110),[3] which demonstrated that although the interfaces are geometrically abrupt and the valence-band edge positions are in good agreement with theoretical predictions, the electronic width of the interface region is 3.5–5.0 nm. This is 3–5 times as large as the results yielded by charge-density contours. In a more recent STS study, concerning InAs thin films on GaAs(111)*A*,[4] it was found that the band gap of the InAs films decreases gradually with film thickness, the proper InAs band gap being established in 3-nm-thick films. Furthermore, the presence of an electron accumulation layer, shown to be a bulk-related effect,[5] is observed in films thicker than 6-nm. This indicates that there is an electronic transition region of 3–6-nm thickness, even though the interface is abrupt. Further studies of such effects are of obvious interest.

Photoemission is well suited for this kind of investigation, since it is one of the most direct methods for probing features of the electronic structure, such as critical points and band edges. The fact that the technique is very surface sensitive is also advantageous in the present context: since the electronic interaction between overlayer and substrate materials is strongest at the interface, the intrinsic properties of the overlayer material should first appear at the surface.

In this work we have studied the development of the interface region in two different systems of thin molecular beam epitaxy (MBE)–grown layers: InAs on GaAs(111)*A* and GaAs on AlAs(100). In the latter case the lattice mismatch is quite small, and the overlayer can be expected to be fully adapted to the substrate for all film thicknesses considered here. The situation for InAs/GaAs is significantly more complex. While growth of InAs on GaAs(100) results in the formation of quantum dots for nominal thicknesses above 2 monolayers (ML), growth on the GaAs(111)*A* surface is two-dimensional (2D) for all overlayer thicknesses. The continuous films formed in this way have been subject to extensive investigations[6–8,4] and have been found to contain a regular network of dislocations, which releases the strain gradually. In the evaluation of the present data we have taken into account the remaining strain found in Ref. 8.

II. EXPERIMENT

The experiments were performed at beamline 41 of the Swedish national synchrotron radiation laboratory MAX-lab in Lund, Sweden. A dedicated MBE system has been attached to the electron spectrometer, allowing transfer between the units under ultrahigh vacuum conditions. The MBE chamber holds five Knudsen-type effusion cells, an As-source (see below), equipment for reflection high-energy electron diffraction (RHEED) and an IR pyrometer. Part of the InAs films were grown with As_4, using a conventional effusion cell, and part with As_2 generated from a valved cracker source. All the GaAs/AlAs experiments employed the As_2 source. Growth was performed on 1×1 cm^2 *n*-type

GaAs(111)*A* and (100)epi-ready substrates, In-glued onto Mo holders.

The InAs layers were grown in the MBE system under conditions similar to those described in literature.[6,7] Prior to growth the substrates were heated to 620–640 °C in a protective As$_4$ (As$_2$) beam to remove the residual surface oxide. Upon appearance of a clear 2D RHEED 2×2 reconstruction pattern, the temperature was lowered to 540–580 °C. To obtain an abrupt interface with InAs, an atomically flat surface is needed and this was achieved by careful buffer layer preparation. GaAs homoepitaxy was performed with an As$_4$:Ga flux ratio in the range (15–20):1 (12:1 for As$_2$). A few hundred nanometers were grown until good quality 2D RHEED patterns were observed. The buffer layer growth on the GaAs(111)*A* surface was followed by InAs deposition at 440–460 °C at an As$_4$:In flux ratio of about (25–40):1 (15:1 for As$_2$). Good quality 2D RHEED patterns of the 2×2 reconstructed surface were observed all the time, although the intensity dropped significantly at the onset of InAs growth and then gradually recovered. The In beam flux was calibrated by measurements of RHEED intensity oscillations during growth of In$_x$Ga$_{1-x}$As on GaAs(100), and the InAs growth rate was determined via RHEED oscillations during growth of a thick InAs film on GaAs(111)*A*. For most samples one or two RHEED oscillations could be seen at the onset of InAs growth. In the present experiments the InAs growth rate was 0.1 ML/s. After the spectroscopic analysis the InAs layer thicknesses were also checked *ex situ* using static secondary ion mass spectroscopy (SIMS), with 6.4-keV (O$_2$)$^+$ ions at a sputtering rate of 0.07 nm/s, and Tallystep profiling of the SIMS-generated pits. The agreement of these results with the original estimations was satisfactory.

In the case of GaAs/AlAs(100), buffer layer growth of about 10-nm GaAs on the GaAs(100) crystals was followed by deposition of 10–20-nm-thick AlAs layers, at a substrate temperature of 570 °C and a growth rate of 0.1 ML/s. The AlAs layers then served as substrates for the thin films of GaAs. The GaAs growth was performed at a substrate temperature of 580 °C and at an As$_2$/Ga beam equivalent pressure ratio of about 10, resulting in a growth rate of 0.25 ML/s (calibrated by RHEED oscillations). The surface reconstruction was 2×4 during growth, changing to $c(4×4)$ when the sample was cooled below about 520 °C in an As$_2$ beam.

In the photoelectron chamber the InAs films were annealed at 250 °C in order to remove excess As adsorbed after growth. The GaAs films were heated to above 400 °C in order to remove excess As and to ensure a $c(2×8)$ reconstruction of the surface. The surface quality was checked by low-energy electron defraction (LEED), which also served to orient the samples.

The photoemission data were collected in the *p*-polarization geometry, at 45° incidence angle, using an angle-resolving, goniometer-mounted, hemispherical electrostatic energy analyzer with an acceptance angle of ∼3°, movable in the horizontal and vertical planes. The overall energy resolution was 0.15–0.25 eV. All spectra presented in this paper were collected in the plane of light incidence.
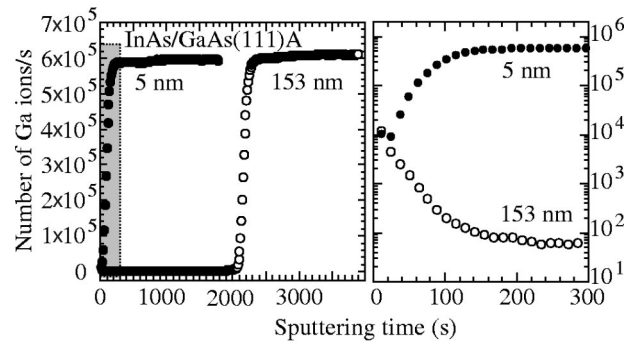
FIG. 1. SIMS data from 5- and 153-nm-thick InAs layers on GaAs(111)*A*, showing the onset of Ga emission from the substrate. The shaded region to the left is also given in an expanded view, on a logarithmic vertical scale, indicating the presence of Ga in the surface region.

III. RESULTS AND DISCUSSION

We first discuss the results for InAs/GaAs(111)*A*. Despite the large lattice mismatch, more than 7%, investigations have shown that growth of InAs on GaAs(111)*A* proceeds in a 2D mode,[7] the overlayer relaxation saturating at a thickness of approximately 10 ML (3.5 nm).[8] These reports were confirmed in our case by RHEED and LEED observations. Streaky 2×2 RHEED patterns were observed for all thicknesses, indicative of a smooth surface. By monitoring the separation of the diffracted streaks during growth we found that gradual strain relaxation occurred up to about 3-nm InAs thickness, above which all samples displayed well-ordered 2×2 reconstructed surfaces, and no significant further strain relaxation seemed to take place. After growth the well-ordered 2×2 surface geometry was confirmed by a good quality LEED pattern. Furthermore, the valence-band photoemission showed very pronounced angular dependence, also revealing good quality single-crystal samples.

The SIMS measurements, performed to check the InAs growth-rate calibration, also addressed the important question of possible segregation of Ga in the InAs films and indeed indicate the presence of Ga in the surface region (see Fig. 1). The SIMS data cannot give reliable estimates of the absolute amounts of Ga but the surface Ga content is similar for all samples. The presence of Ga at the surface was confirmed by core-level photoemission. By recording the spectra at 135 eV photon energy, near the Cooper minimum of In 4*d*,[9] the magnitude of the Ga 3*d* signal could be easily estimated despite the fact that the In 4*d* and Ga 3*d* emission overlap to a large degree (at 81 eV photon energy the Ga 3*d* signal is visible only for the thinnest films). Using a curve-fitting routine, in which the core levels are described by convoluted Gaussian and Lorentzian functions (accounting primarily for experimental and lifetime broadening, respectively), two Ga components were identified. We associate them with Ga dissolved in the uppermost InAs layers and Ga in metallic clusters on the surface (see Fig. 2). The metallic component, characteristically at higher kinetic energy,[10] is present in films several hundred nanometers thick, whereas the other component is restricted to films at most a few hundred ångströms thick. From the relative in-
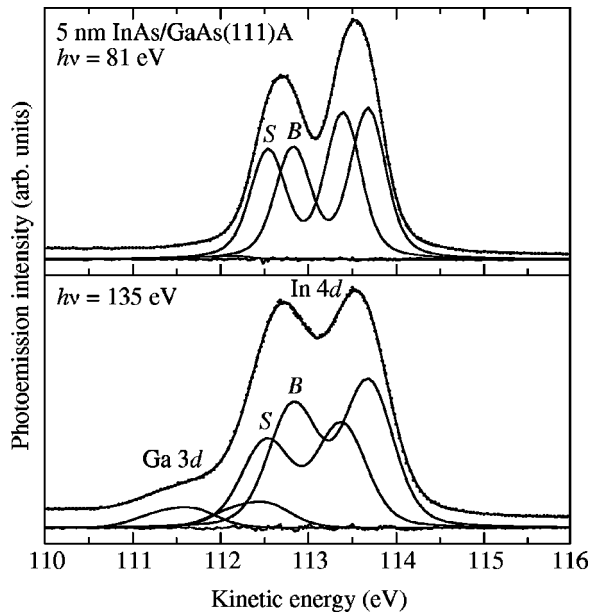
FIG. 2. In $4d$ spectra from a 5-nm-thick InAs layer recorded at 81 eV photon energy and at 135 eV photon energy (near the In $4d$ Cooper minimum). In the latter case the emission from Ga $3d$ is clearly visible. The two Ga components reflect Ga in metallic form (the high-energy component) and Ga dissolved in the surface region of the InAs films. Fitting parameters: In $4d$, $\Delta E_{\text{s-o}}=0.855$ eV, $\Delta E_{\text{Lor}}=0.17$ eV, $\Delta E_{\text{Gauss}}=0.377$ eV ($h\nu=81$ eV) and 0.57 eV ($h\nu=135$ eV), branching ratio$=1.356$ and 1.200, respectively; Ga $3d$, $\Delta E_{\text{s-o}}=0.44$ eV, $\Delta E_{\text{Lor}}=0.14$ eV, $\Delta E_{\text{Gauss}}=0.57$ eV, branching ratio$=1.500$.

tensity of these components and the In $4d$ signal, taking into account the vastly different photoexcitation cross sections at this photon energy,[9] the total Ga content in the surface region was estimated to be below 1%. We believe that these amounts are not sufficiently large to influence essentially the bulk electronic structure discussed below.

In Fig. 3 we show four sets of valence-band data, obtained from the clean GaAs(111)A surface and from three different InAs overlayers. The valence-band spectra reported here were recorded along the $\overline{\Gamma K}$ line in the surface Brillouin zone. The qualitative electronic similarities between GaAs and InAs are well reflected in the spectra, although due to the large difference in lattice constants, spectra at corresponding angles probe slightly different regions of the Brillouin zones in the two cases. By comparison of spectra recorded at the same in-plane momentum component, we were able to conclude that most of the pronounced structures observed on the (111) surface (for example peak C) reflect surface states. Comparing the clean GaAs spectra and those for 1-nm InAs (i.e., around 3 ML) we see that the peak positions are somewhat different. For instance, we find that the energy separation between peaks B (B') and C (C') at $\sim 25°$ emission angle is reduced from 2.2 eV to 1.9 eV when going from clean GaAs to the InAs overlayer system. This separation is reduced further to 1.8 eV in the thicker InAs films. We also see that with increasing InAs thickness the structures B' and C' become sharper. For bulk states (for example peak B') such sharpening is an effect of increasing coherence length,

both in the initial and final states in the photoemission process. For surface states (peak C') the sharpening can be caused by reduced hybridization with bulk states, as the bulk band edges become better defined.

Even though already the 2-nm spectra are very similar to the spectra from the thick InAs overlayer (see Fig. 3), a significant observation in these sets of data is a systematic change of peak positions with increasing thickness. We have chosen to exemplify this by the energy separation between peak A', reflecting the high density of states at the L_1 critical point, and the spectral cutoff at high kinetic energies, which reflects the valence-band maximum (VBM). Both features are thus bulk related. This energy difference is plotted as a function of InAs layer thickness in Fig. 4. A systematic reduction of the energy separation between L_1 and the VBM is clear, and a saturation value appears to be reached for about 5–6-nm thickness.

In order to estimate to what extent these modifications are caused by the gradually decreasing strain within the InAs layer, calculations of the electronic structure in strained InAs were performed. Since the expanding of the InAs cap layer makes any full-scale *ab initio* simulation very difficult (the use of slab supercells is impossible), the calculations assumed a bulk InAs crystal compressed in two dimensions. We thus ignore the effects of interface hybridization and assume also that any influence of effects specific to the strain gradient can be ignored.

To model the bulk compression, we employed *ab initio* density functional theory (DFT),[11,12] within the local density approximation (LDA) as parametrized by Ceperley and Alder[13] and Perdew and Zunger.[14] Fully separable, nonlocal pseudopotentials[15,16] were used for the electron-ion interaction, based on self-consistent solutions of the relativistic Dirac equation for free atoms.[17–19] The strained system was described by periodically repeated hexagonal supercells with three double InAs atomic layers stacked in a face-centered-cubic type layer sequence along the (111) axis. A plane-wave cutoff of 16 Ry and 23 special Monkhorst-Pack **k** points in the irreducible Brillouin zone were used to sample the wave functions in the supercells, corresponding to 128 points in the full zone.

The xy plane was held fixed for different compressions, while the periodic distance for the z axis was optimized with respect to the total energy. All atoms were free to relax to their equilibrium positions in each case. For zero compression, the ideal undistorted zinc-blende geometry and InAs electronic structure was retrieved with the theoretical lattice constant of 6.06 Å, which coincides with the experimental one. All atomic forces were converged to 0.005 eV/Å and the total numerical uncertainty for the geometrical optimization was estimated to 0.03 Å. The uncertainty in the resulting electronic structure was found to be well below 0.05 eV.

Considering first the geometrical results we notice that the compression gives a relatively modest increase in the length of the periodicity along the (111) axis, to a maximum of about 4% for fully compressed cells (a constant-volume approximation gives a value of $\sim 15\%$). The dependence on the degree of relaxation is very nearly linear. The conservation of bond lengths and volume results in forces acting to-
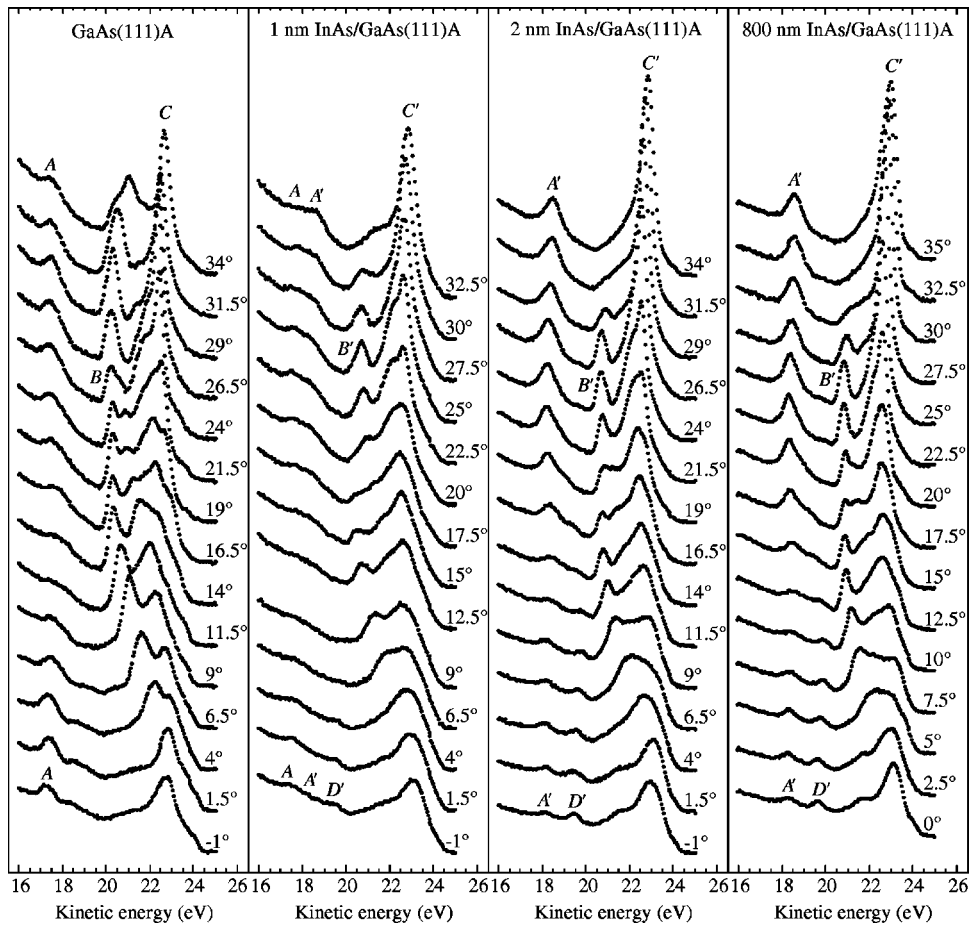
FIG. 3. A comparison between valence-band spectra recorded at different emission angles from the clean GaAs(111)*A* surface and from InAs overlayers of 1-, 2-, and 800-nm thickness. The spectra were excited with 29-eV photons and recorded along the $\overline{\Gamma K}$ line in the surface Brillouin zone. Labels *A* (*A'*) and *B* (*B'*) denote bulk states, and *C* (*C'*) and *D'* surface states.

wards prolonging the distance between periodic boundaries, but the *sp* hybridization is also striving to conserve the bond angles and this keeps down the *z*-axis periodic distance. The electrostatic forces due to the polar nature of InAs also act towards contraction. Hence the quantum mechanical angular and electrostatic forces act in the opposite direction to the semiclassical ones, and the *z* expansion is a result of this balance. Considering its widespread use, it is interesting to note how poorly the constant-volume approximation predicts the *z*-axis values for compressed cells [it gives values almost

four times too large for the increase of the lattice constant in the (111) direction].

Turning to the effects of the in-plane compression on the electronic structure (see Fig. 5), we observe that the energy separation ΔE between the L_1 and X_1 critical points and the VBM decreases with increasing relaxation (i.e., increasing thickness). It should be noted that while the fundamental
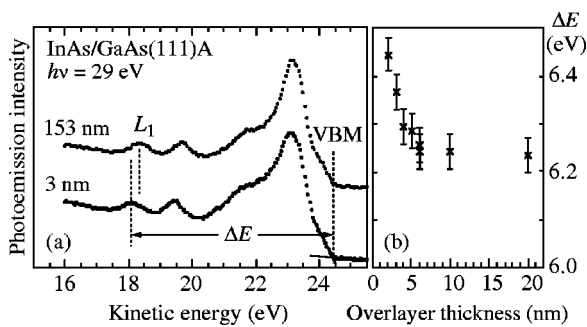
FIG. 4. (a) Normal emission valence-band spectra from 3- and 153-nm InAs layers on GaAs(111)*A*, obtained with 29-eV photons. (b) The energy difference between the density of states peak at the L_1 critical point (feature *A'* in Fig. 3) and the VBM [as indicated in (a)] as a function of InAs layer thickness.
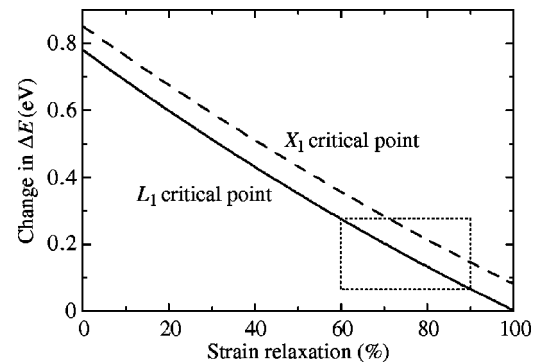
FIG. 5. Strain effects calculations on bulk InAs. The solid (dashed) line represents the change in energy separation, ΔE, between the VBM and the L_1 (X_1) critical point with varying strain (as described in the text). The region indicated by the rectangle shows the approximate range of the theoretical data used in the comparison in Fig. 6 between strain effects and interface hybridization.
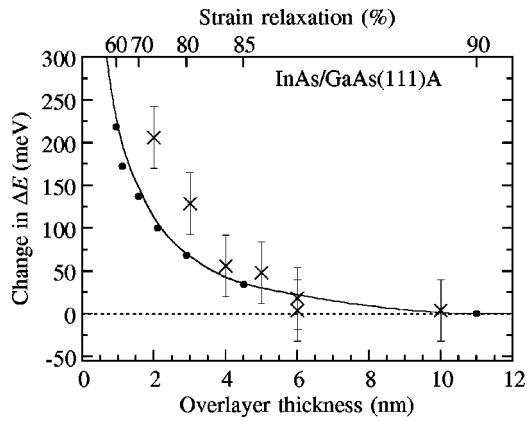
FIG. 6. A comparison between the experimental data in Fig. 4(b) and the calculated influence of compression on bulk InAs electronic structure. The theoretical and experimental data are plotted using the energy separation between L_1 and the VBM at 90% strain relaxation as a common zero. The change in energy separation is plotted against both overlayer thickness (lower x axis) and strain relaxation (upper x axis), related to each other using Ref. 8. The filled circles represent theoretical data and are joined by a smoothed interpolated line.

band gap is underestimated in DFT-LDA, the bandwidth of the occupied states should be free of such effects, and in particular, the movements of the L_1 and X_1 critical points should be adequately reproduced.

By fitting the theoretical findings to the experimentally measured compression, using the observed relationship between strain relaxation and overlayer thickness reported in Ref. 8, it now becomes possible to compare the compression-induced movement of the L_1 critical point and the influence from interface hybridization (see Fig. 6). It is assumed that the saturation value of the energy separation between L_1 and the VBM in Fig. 4 corresponds to a strain relaxation of $\sim 90\%$ (as reported in Ref. 8). The calculated movement of the L_1 point in compressed bulk InAs and the experimental data on the cap layers agree well, down to about 4 nm from the interface. At smaller thicknesses the effect of interface hybridization is clearly seen as the experimental points move away from the theoretical line of pure compression effects. Hence, the non-strain-related influence from the interface on the electronic structure extends 3–4 nm into the overlayer, while strain effects modify the valence-band structure for an additional 1–2 nm. We ascribe these changes in the width of the valence band to the gradual development of the overlayer valence-band structure and thus conclude that full InAs bulk features are established only in films of more than 3–4-nm thickness.

A unique feature of InAs that independently supports this statement is the development of a charge accumulation layer in the surface region. The presence of charge accumulation at free InAs surfaces has been shown to be a bulk-related effect,[5] due to a narrow minimum in the lowest conduction band at the center of the Brillouin zone. When this band is fully developed, the minimum becomes populated and can be observed in photoemission as a small peak just above the VBM (see Fig. 7). Indeed, we find that photoemission from
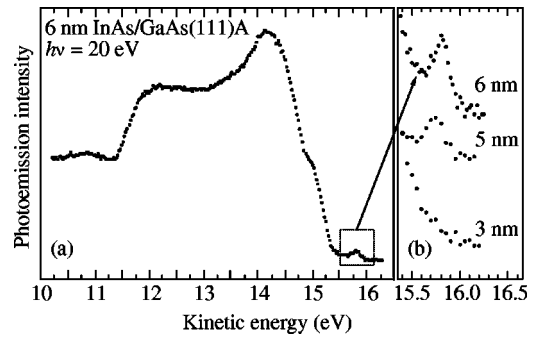
FIG. 7. (a) A normal emission valence-band spectrum from a 6-nm-thick InAs film obtained at 20 eV photon energy. Note the presence of charge-accumulation-layer emission. (b) An enlargement of the indicated region in (a), with data from 3- and 5-nm-thick films included.

the conduction band is present only in layers of a thickness of ~ 5 nm or more, confirming that the bulk InAs valence-band structure is not fully developed for thinner samples. This agrees well with the observations in Ref. 4.

Turning to the GaAs/AlAs(100) system, the MBE growth of these quite well lattice-matched materials is firmly established and the samples show characteristic 2D RHEED features for all thicknesses. Monitoring the peak value of the absolute intensity of the Al $2p$ signal (see Fig. 8), we find an electron mean free path of about 7 Å at 27 eV kinetic energy in the GaAs films. This is in good agreement with literature.[20] The as-grown samples all displayed the $c(4 \times 4)$ reconstruction. In the photoemission chamber they were heated to remove excess As to reach the $c(2 \times 8)$ reconstruction. Photoemission measurements were performed, however, both on surfaces with a clear $c(2 \times 8)$ reconstruction and on surfaces ranging between $c(4 \times 4)$ and $c(2 \times 8)$ reconstructions. To minimize potential complications due to somewhat varying surface geometry we only discuss
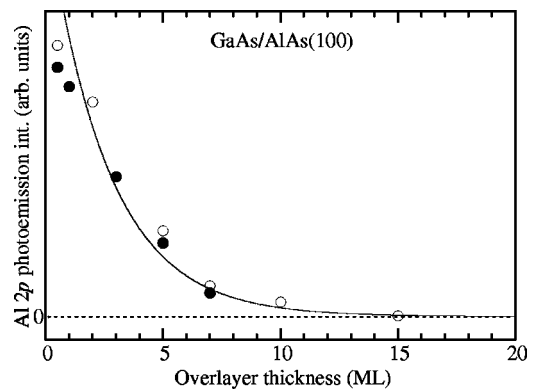
FIG. 8. The Al $2p$ normal emission intensity, excited with 105-eV photons, as a function of GaAs overlayer thickness. Filled circles mark surfaces with somewhat higher As content. Two data points for the same thickness means that measurements were performed on the same sample before and after heating. The solid line indicates an exponential fit, yielding an electron mean free path of about 7 Å ($\lambda \approx 2.60$ ML = 7.3 Å) in the GaAs films for 27 eV kinetic energy.
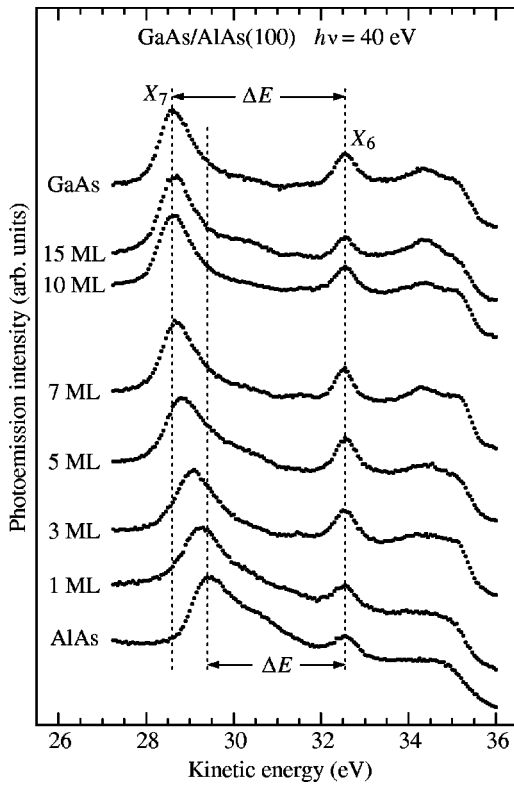
FIG. 9. Normal emission valence-band spectra from clean AlAs, GaAs, and 1–15-ML-thick GaAs layers on AlAs(100), obtained with 40-eV photons. The spectra were aligned at the X_6 density of states peak.

FIG. 10. The energy difference between the X_6 and X_7 density of states peaks (as indicated in Fig. 9) as a function of GaAs layer thickness. As the width and shape of the X_7 peak vary somewhat for different spectra, the relative peak position was determined by matching the spectra at the left flank of the X_7 peak, using the pure AlAs spectrum at the bottom of Fig. 9 as a reference. Filled circles mark surfaces with somewhat higher As content. Two data points for the same thickness means that measurements were performed on the same sample before and after heating, except in the cases of 10-ML thickness, in which case two different samples were examined.

normal emission spectra in the following and focus on bulk-induced features. The surface conditions were checked by LEED and the As content was also reflected by the shape of the As $3d$ core-level photoemission. The shape of the valence-band spectra differed slightly between samples with different surface reconstructions, but as we shall focus on bulk-induced structures, we do not comment further on these differences.

As seen in Fig. 9, the valence-band spectra of AlAs and GaAs, recorded at a photon energy of 40 eV, are very similar, both dominated by the pronounced density of states peaks at the X_6 and X_7 critical points. The kinetic energy of the emission from the X_6 points is about the same for both materials in our spectra. The position of the peak corresponding to the X_7 point, however, is about 0.8 eV lower in GaAs. We have chosen the separation between the X_6 and X_7 peaks as a characteristic measure of the valence-band character. A systematic study of 1–15-ML-thick GaAs films on AlAs shows that the X_7 peak gradually shifts to lower kinetic energy with increasing layer thickness, reaching the position in bulk GaAs at about 7–10-ML thickness ($\sim 2-3$ nm). Two 20-ML samples were also grown, but Al $2p$ emission was visible in photoemission, indicating either that the substrate is laid bare at places or that the surface is contaminated with Al. No spectra from any of these defect samples are included in Fig. 9, but they fall in well with the peak positions in the 15-ML and pure GaAs spectra. To check that the

shifting peak is not an artifact caused by the superposition of two separate peaks with varying relative intensities, we have generated such superimposed spectra from bulk AlAs and GaAs data. The result differed markedly from the real data in Fig. 9. In all the composed spectra the GaAs and AlAs X_7 peaks appear as separate features, without giving the impression of a continuously shifting structure.

The energy separation between the X_6 and X_7 peaks, ΔE, is plotted as a function of overlayer thickness in Fig. 10. Similar to the InAs/GaAs(111)A case, we find that the electronic interface region of the GaAs films spans ~ 3 nm.

Effects of this kind have also been discussed in context with photoluminescence (PL) from GaAs/AlAs QWs and superlattices. As a result of electronic coupling across an AlAs barrier one finds,[1] for example, that PL spectra from GaAs QWs are shifted for barrier widths below ~ 3 nm. The Γ subband energies are lowered due to this coupling, and the band alignment is eventually changed from type II to type I at 10–15-Å barrier width. The tunneling of GaAs QW states through an AlAs barrier has also been found[2] to affect the PL intensity when the barrier thickness in less than about 4 nm. Both these results are in fair agreement with the present observations.

IV. CONCLUSIONS

We interpret the observed systematic variations in valence-band width as an effect of electronic states tailing across the interface within a range of about 3–4 nm. In the case of the highly-lattice-mismatched InAs/GaAs system, strain effects must be taken into account to estimate the range of the electronic transition region. In this region the electrons thus experience an average potential from the substrate and overlayer materials, resulting in alloylike proper-

ties. The fact that the transition region of the electronic properties is substantially larger than that of the geometrical structure should have implications for nm-scale device design and fabrication. A recent example of this is a study of the coupling between vertically stacked $In_{0.1}Ga_{0.9}As$ quantum-wire structures in GaAs.[21] According to this study clear electronic coupling effects between different wires are observed for GaAs barriers thinner than approximately 10 nm, which would mean that the QW states extend at least ~ 5 nm across the $In_{0.1}Ga_{0.9}As$/GaAs interface.

[1] K.J. Moore, P. Dawson, and C.T. Foxon, Phys. Rev. B **38**, 3368 (1988).

[2] T. Tada, A. Yamaguchi, T. Ninomiya, H. Uchiki, T. Kobayashi, and T. Yao, J. Appl. Phys. **63**, 5491 (1988).

[3] H.W.M. Salemink, O. Albrektsen, and P. Koenraad, Phys. Rev. B **45**, 6946 (1992).

[4] H. Yamaguchi, J.L. Sudijono, B.A. Joyce, T.S. Jones, C. Gatzke, and R.A. Stradling, Phys. Rev. B **58**, R4219 (1998).

[5] L.Ö. Olsson, C.B.M. Andersson, M.C. Håkansson, J. Kanski, L. Ilver, and U.O. Karlsson, Phys. Rev. Lett. **76**, 3626 (1996).

[6] K. Sato, M.R. Fahy, and B.A. Joyce, Surf. Sci. **315**, 105 (1994).

[7] H. Yamaguchi, M.R. Fahy, and B.A. Joyce, Appl. Phys. Lett. **69**, 776 (1996).

[8] H. Yamaguchi, J.G. Belk, X.M. Zhang, J.L. Sudijono, M.R. Fahy, T.S. Jones, D.W. Pashley, and B.A. Joyce, Phys. Rev. B **55**, 1337 (1997).

[9] J.J. Yeh and I. Lindau, At. Data Nucl. Data Tables **32**, 1 (1985).

[10] G. Le Lay, D. Mao, A. Kahn, Y. Hwu, and G. Margaritondo, Phys. Rev. B **43**, 14 301 (1991).

[11] W. Kohn and L.J. Sham, Phys. Rev. **140**, A1133 (1965).

[12] P. Hohenberg and W. Kohn, Phys. Rev. **136**, B864 (1964).

[13] D.M. Ceperley and B.J. Alder, Phys. Rev. Lett. **45**, 566 (1980).

[14] J.P. Perdew and A. Zunger, Phys. Rev. B **23**, 5048 (1981).

[15] D.R. Hamann, Phys. Rev. B **40**, 2980 (1989).

[16] X. Gonze, P. Käckell, and M. Scheffler, Phys. Rev. B **41**, 12 264 (1990).

[17] D.R. Hamann, M. Schlüter, and C. Chiang, Phys. Rev. Lett. **43**, 1494 (1979).

[18] G.B. Bachelet, D.R. Hamann, and M. Schlüter, Phys. Rev. B **26**, 4199 (1982).

[19] L. Kleinman and D.M. Bylander, Phys. Rev. Lett. **48**, 1425 (1982).

[20] W. Mönch, *Semiconductor Surfaces and Interfaces*, 2nd ed., Vol. 26 of Springer Series in Surface Science (Springer, Berlin, 1995), p. 9, and references therein.

[21] R. Rinaldi, M. De Giorgi, A. Passaseo, R. Cingolani, R. Ferreira, and G. Bastard, in *Proceedings of the 24th International Conference on the Physics of Semiconductors*, edited by D. Gershoni (World Scientific, Singapore, 1999), 1189.PDF.